

The response of semi-arid ephemeral wetland plants to flooding: linking water use to hydrological processes

Paul L. Drake,^{1*} Blaire F. Coleman¹ and Ryan Vogwill^{1,2}

¹ Natural Resources Branch, Department of Environment and Conservation, Locked Bag 104, Bentley Delivery Centre, WA, 6983, Australia

² School of Earth and Environment, University of Western Australia, Hackett Drive, Nedlands, WA, 6009, Australia

ABSTRACT

Evergreen plants inhabiting ephemeral wetlands endure long dry spells interspersed with periods of flooding (or inundation). Inundation events are likely to be important for plant water use and growth, but few studies have linked the physiology of plants to hydrological processes during flood. We investigated the link between changes in the soil physical environment and plant water use traits in a stand of *Casuarina obesa* Miq and *Melaleuca strobophylla* Barlow trees during a controlled inundation event at Toolibin Lake. Toolibin Lake is an internationally recognized ephemeral wetland, which is under threat from altered hydrology and salinization. During flood, the velocity of water movement through the clay-dominated soil profile suggested that macropores and plant root preferential flow paths aided water distribution. *C. obesa* was more capable than *M. strobophylla* to capitalize on the inundation event, suggesting preferential use of macropore water and a concentration of roots near the soil surface. Sap flux (Q_s) and tree diameter (ϕ) were interdependent and there was a correlation between increasing ϕ and increasing pre-dawn leaf water potential (Ψ_{pd}). These observations link the movement of water through the soil profile with changes in tree water use and tree girth in *C. obesa* and *M. strobophylla*. Changes in the soil physical environment observed in this study also highlight the risks associated with hydrological management in salinity-affected ecosystems. Although floods provide fresh water to the root zone of trees, the resulting recharge may also elevate saline groundwater into the region of plant water uptake. Copyright © 2012 State of Western Australia

KEY WORDS dendrometer; groundwater; infiltration; macropores; salinity; transpiration; water potential

Received 27 February 2012; Revised 9 July 2012; Accepted 26 July 2012

INTRODUCTION

Ephemeral and seasonal wetlands in semi-arid regions are highly dynamic habitats (Whigham, 1999; Touchette *et al.*, 2010). As a result, the dominant plant species of these areas are well adapted to rapid changes in wetland abiotic properties. Evergreen plants of semi-arid ephemeral wetlands, for example, will typically endure long dry spells punctuated by short wet periods. Evergreen plants must respond quickly to capitalize on these short wet periods. In reference to stomatal control strategies, this may manifest as rapid opening and an increase in both stomatal conductance to water vapour (g_w) and transpiration rate (E). A higher g_w will be associated with a higher stomatal conductance to CO₂ (g_c) and this, in turn, will usually sustain a higher rate of photosynthetic carbon uptake (A) (Cowan, 1977; Farquhar and Sharkey, 1982). Hence, the episodic inundation events that characterize ephemeral wetlands are likely to influence plant biomass accumulation. However, little is known about how rapidly evergreen plants of ephemeral wetlands modify their water use in response to inundation and whether this change is directly related to biomass accumulation.

The distribution of plants in wetland ecosystems is strongly influenced by hydrological processes (Neill, 1990; Fennessy *et al.*, 1994), and this is primarily due to inherent limitations of root anatomy and physiology (Sorrell *et al.*, 2000). Inter-specific differences in ability to form aerenchyma tissue to maintain aerobic respiration during prolonged water logging (Kawase, 1981), for example, can influence the spatial distribution of emergent macrophytes along a hydrological gradient (Tornbjerg *et al.*, 1994). Further, species' root distributions may determine their survival during prolonged dry spells (Jackson *et al.*, 1999), which are typical of semi-arid ephemeral wetlands. The inherent properties of roots in ephemeral wetland species will therefore determine their water use and growth traits during phases of drought and surface water inundation.

Toolibin Lake, an ephemeral wetland of semi-arid south western Australia, is dominated by two morphologically distinct evergreen species: *Casuarina obesa* Miq. and *Melaleuca strobophylla* Barlow, which co-occur in dense thickets. *C. obesa*, a dioecious tree with needle-like, photosynthetically active branchlets (cladodes), is highly tolerant of inundation, drought and soil salinity (El-Lakany and Luard, 1983; Bell, 1999). *M. strobophylla*, a 'paperbark' tree with small obovate leaves, is thought to be moderately tolerant of inundation, drought and soil salinity on the basis of the performance of closely related species (Bell, 1999). On a seasonal basis, these species will typically acquire water from rainfall incident upon the lake bed.

*Correspondence to: Paul L. Drake, Natural Resources Branch, Department of Environment and Conservation, Locked Bag 104, Bentley Delivery Centre, WA 6983, Australia.
E-mail: paul.drake@dec.wa.gov.au

However, ephemeral floods are likely to alter the soil abiotic environment in a different manner to water inputs from average annual rainfall. The response of these species to such flood events, in terms of water use and tree girth, is the focus of this study.

Toolibin Lake is one of the last remaining fresh to brackish wetlands in the region, and the lake bed biota is under threat from altered hydrology and salinization (secondary salinity). The lake is listed as a Wetland of International Importance under the Ramsar Convention. Land clearing and associated hydrological changes have caused salt to mobilize (George *et al.*, 1997), and this is entering the lake as episodic saline surface water inflows and rising saline groundwater. To limit the impacts of secondary salinity, the managing authority regulates the amount, and quality of surface water entering the lake and the depth of groundwater beneath the lake using, respectively, a diversion channel and a network of groundwater pumps. In the last decade, the management criterion for water quality at the lake inlet (less than 1000 mg l⁻¹ of total dissolved salts) has rarely been met, and as a result, the lake bed has remained largely free of surface water for an extended period. To understand how the two dominant tree species of the lake respond to surface water, we simulated an inundation event in a stand of *C. obesa* and *M. strobophylla*. We hypothesized that, in relation to water use and tree girth, the two species would respond differently to inundation because of their contrasting morphological and physiological properties. Specifically, we predicted that *C. obesa* roots occupied shallow soil layers and *M. strobophylla* roots occupied relatively deep soil layers, and that these different architectural arrangements would influence changes in tree girth and water use during both flooding and periods of prolonged water stress. Our aim was to demonstrate that the changes in water use and tree girth in the two tree species during flood is a function of root architecture and changes to the physical properties of the soil profile.

MATERIAL AND METHODS

Study site

All measurements were carried out at Toolibin Lake (556800 E; 6357400 N), an ephemeral wetland covering an area of approximately 300 ha. The lake is located in the upper reaches of the Blackwood River catchment in south western Australia. Average annual rainfall between 1912 and 2010 was 408 mm with the majority falling between May and August when temperatures were, on average, lowest (Australian Bureau of Meteorology, 2010). Annual average evaporation during the same period was 1688 mm (Australian Bureau of Meteorology, 2010). Most of the Toolibin Lake catchment was cleared of native vegetation and converted to annual agricultural crops and pastures during the last 100 years. The soils of the Toolibin Lake bed are dominated by clay and clay loam overlain by a thin organic A-horizon of less than 10 cm. The deep clay and clay loam sediments include a small fraction of sand and gravel that shows heterogeneity in both vertical and horizontal planes.

The groundwater beneath Toolibin Lake is typically within 3 m of the soil surface and has a salinity in excess of 30000 mg l⁻¹ total dissolved salts (or an electrical conductivity, EC, of approximately 55 mS cm⁻¹ assuming that NaCl is the dominant salt in solution). Surface water flows into Toolibin Lake are highly variable in both volume and salt load (George and Dogramaci, 2000). Installation of a separator gate and diversion channel in 1995 has enabled managers to exclude highly saline low volume inflows. A network of groundwater pumps is positioned on the lake bed to lower groundwater beneath trees. This regulated environment provides an ideal opportunity to test the response of semi-arid wetland plants to a simulated inundation event.

Two 20 m × 20 m experimental plots were established in a thicket of *C. obesa* and *M. strobophylla*, approximately 80 m apart (Fig. 1). The first plot served as a control and was not inundated during the experiment. The second plot was subdivided into an area that was not inundated (termed 'outside') and an area that was inundated (termed 'inundated') (Fig. 1). The terms 'inundated' and 'flooded' are used to indicate that standing water was present on the soil surface. The inundated area was bordered by a rectangular bund constructed from sand bags and polymer

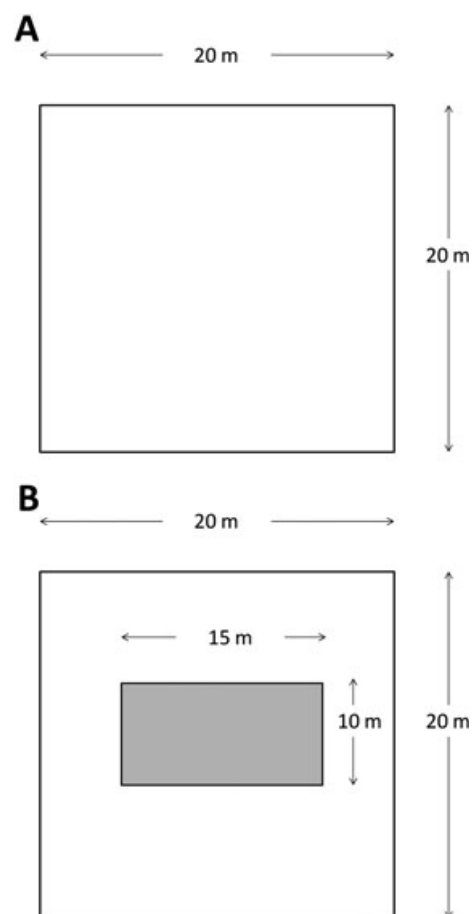


Figure 1. Schematic diagram of the design of the experiment depicting control (A), outside and inundated (B) plots. The inundated plot was boarded by a sandbag bund, which was 15 m long by 10 m wide by 0.5 m high (the shaded area). The outside plot was immediately external to the inundated area.

film (15 m long by 10 m wide by 0.5 m high). Tree density was 1525, 11280 and 8267 stems per hectare (sph) for the control, outside and inundated plots, respectively. The different densities of trees did not equate to a large difference in plot-scale sap wood area (see following paragraphs) because the control plot comprised larger trees, and hence more sap wood per stem.

At 9:00 am on Tuesday, 22 March 2011, fresh water was gravity fed into the bund from two 9500-L tanks that were replenished by a water truck throughout the day. The water was distributed over the surface of the bund area by three 5-m lengths of slotted tube. Over the course of the day, approximately 60000 l of water was applied. An additional 20000 l was delivered on Friday, 25 March 2011, and a further 10000 l was delivered on Friday, 1 April 2011 and Tuesday, 5 April 2011, making a total of 100000 l. Surface water was maintained in the inundated plot for 35 days and during this period, 9.8 mm of rainfall was detected, and the average maximum daily temperature was 27 °C (Fig. 2). In the 50 days prior to inundation, only 1.8 mm of rainfall was detected and over this same period, the average maximum daily temperature was 30 °C (Fig. 2).

Climate

A weather station (Model U30-NRC, Onset, Bourne, USA) was erected approximately 500 m from the experiment in a clearing more than two canopy heights from the nearest tree. The weather station was equipped with a tipping bucket rain gauge, a radiation sensor, a temperature and humidity sensor, an anemometer and wind direction sensor. The weather station was set to log climatic data at 30-min intervals. We used the climatic data obtained from the meteorological instruments to estimate daily potential evapotranspiration (or reference crop evapotranspiration, ET_0 , mm) according to Allen *et al.* (1998). This method uses climatic factors to estimate the evapotranspiration rate from a reference surface, a hypothetical grass reference crop with specific characteristics.

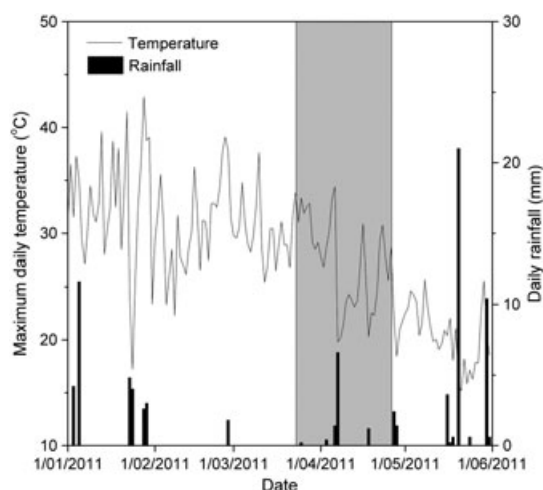


Figure 2. Maximum daily temperature and daily rainfall recorded during the study period from a weather station located on the lake. The shaded band depicts the period that surface water was present in the inundated plot.

Surface water and groundwater

Surface water depth (cm) and surface water electrical conductivity (EC, mS cm^{-1}) were recorded at 15-min intervals with a multi parameter water logger (Model CTD-Diver, Van Essen Instruments, Delft, The Netherlands) that was installed in a length of slotted PVC tubing. Groundwater depth (cm) was also measured at 15-min intervals from a piezometer located in each plot using multi parameter water loggers ($n = 1$ sensor per plot) (Model Cera-Diver, Van Essen Instruments, Delft, The Netherlands). Piezometers were installed using a 90-mm hollow stem auger drill rig. The piezometers were constructed from 50-mm (internal diameter) PVC tubing, with slotted screen sections positioned below the water table. The slotted sections were covered by a filter sock. The annulus was backfilled with gravel over the screened interval and sealed with bentonite before the remainder was filled with drill cuttings and sealed with cement at the surface. Piezometers were installed approximately 23 months before the experiment (at the end of the dry season), and soil samples were collected during installation for determination of soil volumetric water content and soil water potential (θ_v , % and Ψ_{soil} respectively, see following paragraphs). Surface water and groundwater pressure measurements were compensated for barometric pressure using a pressure sensor positioned on the lake bed (Model Baro-Diver, Van Essen Instruments, Delft, The Netherlands). Surface water and groundwater depths were also recorded manually throughout the experiment to verify logged data.

Soil moisture and soil water potential

Soil moisture was recorded at 15-min intervals as θ_v , %, using high frequency theta probes (Model MP406, ICT International, Armidale, Australia) in the control and inundated plots. The theta probes were connected to a digital interface (Model SMD4-P, ICT International, Armidale, Australia) and data recorded by a logger (Model SL5, ICT International, Armidale, Australia).

Four probes were deployed in each plot at 0.2, 0.8, 1.6 and 3.0 m from the soil surface using a drill rig as described earlier. The probes were pushed into the undisturbed soil through the open end of 50-mm (internal diameter) PVC tubing, which was then sealed at the top. The annulus was then backfilled with soil cuttings and bentonite, and sealed with cement to reduce the likelihood of preferential water movement. The probes were installed 23 months prior to the experiment, and soil samples ($n = 4$ samples per depth increment for each plot) were collected during installation to verify volumetric water content (θ_v , %) at the probe depths and to characterize soil water potential (Ψ_{soil} , MPa) through the soil profile. Soil samples were sealed in acrylic tubes, refrigerated and transported to a laboratory where half of each sample was used to measure θ_v with the remainder used to measure Ψ_{soil} . For determination of θ_v , soil dry weight was obtained by oven drying at 105 °C for 48 h. The difference between θ_v measured with theta probes and θ_v measured manually was less than 5%. The soil water potential of each sample was measured at 20 °C with a dewpoint potentiometer (model WP4C, Decagon Devices, WA, USA).

Leaf water potential

Pre-dawn leaf water potential (Ψ_{pd} , MPa) was determined from three *C. obesa* trees and three *M. strobophylla* trees in each of the control, outside and inundated plots ($n = 1$ leaf per tree) using a Scholander-type pressure chamber (Model PMS 1000, Plant Moisture Systems, Albany, USA) (Scholander *et al.*, 1964). Ψ_{pd} was determined 12 days prior to inundation, then 2, 8 and 28 days after inundation. On each occasion, leaves from the upper canopy were collected and stored cool in snap lock plastic bags prior to measurement. The low leaf water potentials observed in each species meant that an individual measurement took longer than usual. This necessitated a small sample size to ensure that leaves were not stored for more than 1 h, which could have resulted in an erroneous value for Ψ_{pd} . For each tree, the difference in Ψ_{pd} measured 12 days prior to inundation and 2 days after inundation ($\Delta\Psi$, MPa) was also calculated. Pre-dawn leaf water potential was also determined on the day that soil samples were acquired for measurement of Ψ_{soil} , that is, at the end of the dry season, 23 months prior to the experiment.

Sap flow

Sap velocity was measured at 15-min intervals on the same trees that were sampled for Ψ_{pd} . Trees were selected to cover the range of stem size in each plot so that average stem sap flow could be scaled to the total stem number to give a stand level estimate. We acknowledge that during drought, sap velocity may be driven by convective water transport (Tanner and Beevers, 2001), but we consider sap velocity to be a good approximation of transpiration rate in this study.

Sap velocity was measured using the heat ratio method (HRM) (Burgess *et al.*, 2001) employing one or two heat pulse sensors per tree (Model HRM 30, ICT International, Armidale, Australia), each connected to a digital interface and data recorded by a logger (Model SL5, ICT International, Armidale, Australia). Probes were installed within active sap wood at 1.8 m from the ground surface. The depth of active sap wood was determined by establishing a relationship between sap wood depth (D_s , mm) and diameter at breast height (DBH, cm) from trees in the vicinity of the experiment that ranged in size (Fig. 3A, $D_s = -65.4 + 61.1\text{DBH}^{0.1}$, $R^2 = 0.83$, $P < 0.01$). The interface of sap wood and heart wood in these trees was estimated as the point where a distinct colour change in tree cores was observed. Using the relationship between D_s and DBH, we estimated the depth of active sap wood in each of the trees fitted with heat pulse sensors. We also established a relationship between sap wood area (A_s , cm²) and DBH (Fig. 3B, $A_s = \text{DBH}^{1.5}$, $R^2 = 0.94$, $P < 0.01$) so that the total sap wood area of each plot (A_s , m²) was estimated by measuring the DBH of each tree. Sap flow velocity (V_s , cm h⁻¹) was converted to sap flux (Q_s , m³ h⁻¹ stem⁻¹) using the procedure described by Burgess *et al.* (2001). Sap velocity was corrected for the thermal diffusivity of sapwood (k , cm² s⁻¹), probe misalignment, wounding due to probe installation, sapwood density and sapwood

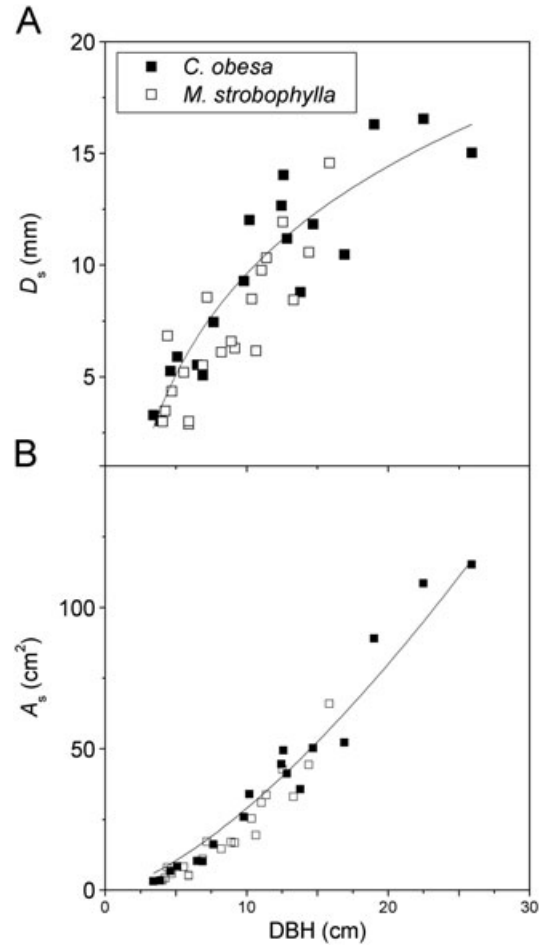


Figure 3. Relationship between sap wood depth (D_s) and diameter at breast height (DBH) (panel A) and sap wood area (A_s) and DBH (panel B) for *Casuarina obesa* and *Melaleuca strobophylla* at Toolibin Lake.

water content. Wound widths were determined as the visual deformation of sap wood in wood cores where sensors had been installed ($n = 5$ for each species). Baseline values for V_s were taken from data recorded overnight after recent rainfall. Following correction, daily Q_s , in m³ day⁻¹ stem⁻¹, was calculated by summing the hourly rates obtained over each 24-h period, and converted to daily stand transpiration rate (E , mm day⁻¹) using the following:

$$E = \left(\frac{\sum_{i=1}^n Q_{s,i}}{\sum_{i=1}^n A_{s,i}} \right) \left(\frac{A_s}{A_{\text{plot}}} \right) \times 1000 \quad (1)$$

where A_s is the total plot sapwood area (m²) derived from the relationship depicted in Fig. 3B, A_{plot} is the total plot area (m²), and $A_{s,i}$ and $Q_{s,i}$ are, respectively, the sapwood area and daily sap flux for the i th of n stems fitted with heat pulse sensors.

Tree diameter

Within the inundation plot, an automatic point dendrometer (Agricultural Electronic Corporation, Tucson, USA) was installed on each tree that was fitted with a heat pulse sensor (three *C. obesa* trees and three *M. strobophylla* trees)

at 1.8 m from the ground surface. A further two automatic point dendrometers were installed on one *C. obesa* tree and one *M. strobophylla* tree outside the inundation plot at 1.8 m from the ground surface, and these were also fitted with heat pulse sensors. Hence, a total of eight trees were fitted with both sap flow sensors and automatic point dendrometers. Each dendrometer was connected to a logger (POD, Agricultural Electronic Corporation, Tucson, USA) and set to record displacement at 30-min intervals. Prior to the experiment, we accurately measured the tree diameter where each point dendrometer made contact with the stem (ϕ) so that the displacement recorded by the dendrometers could be converted to ϕ (assuming that tree girth changed uniformly in all cardinal directions). For each tree, the difference in daily maximum ϕ measured 12 days prior to inundation (ϕ_{-12}) and 2 days after inundation (ϕ_2) was determined and expressed as a function of ϕ_{-12} ($\Delta\phi$, cm cm^{-1}).

Data analysis

Pre-dawn leaf water potential and Q_s data were analysed using a repeated measures ANOVA, and θ_v data were analysed using a two-way ANOVA (MINITAB Version 13, State College, PA, USA) with significance (P) set to 0.05. Comparisons were made between species, treatment and measurement period for Ψ_{pd} and Q_s , and treatment and measurement period for θ_v . The strength of bivariate relationships was quantified as correlation coefficients.

We acknowledge that our design effectively made comparisons against one experimental unit, a single rectangular bund, and this potentially violates the assumption of ANOVAs that all samples are independent (Hurlbert, 1984). However, Oksanen, 2001 argues that use of inferential statistics in a deductive experimental design, such as the present study, is a valid means of testing hypotheses.

RESULTS

Soil and leaf water potential prior to inundation

Soil water potential (Ψ_{soil}), measured from soil cores that were collected 23 months before inundation, ranged from -3.3 to -5.9 MPa (Fig. 4), with the lowest Ψ_{soil} recorded between 50 and 100 cm from the soil surface. On the same day that Ψ_{soil} was determined, there was a distinct separation in pre-dawn leaf water potential (Ψ_{pd}) between *C. obesa* and *M. strobophylla*, represented by the shaded bands in Fig. 4. *C. obesa* had a lower Ψ_{pd} than *M. strobophylla*. The Ψ_{pd} of *C. obesa* leaves matched the Ψ_{soil} of the upper profile, whereas the Ψ_{pd} of *M. strobophylla* leaves was closer to the Ψ_{soil} measured deeper in the profile.

Change in water and soil properties during inundation

During the first day of inundation, the depth of surface water increased at a rate of approximately 9 cm h^{-1} , and the surface water level rapidly declined as inflow ceased when the tank water supply was depleted (Fig. 5A). Subsequent applications of water 3, 10 and 15 days later also resulted in an increase in surface water. After the last application, the

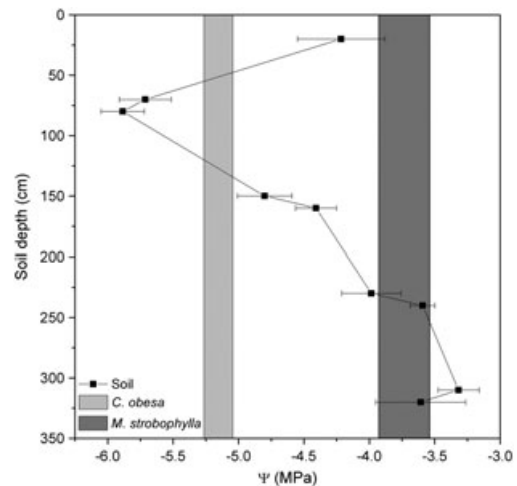


Figure 4. Mean (\pm s. e.) soil water potential (Ψ_{soil}) through the profile at Toolibin Lake at the end of the dry season in 2009, 23 months prior to the inundation trial. The range of pre-dawn leaf water potential (Ψ_{pd}) for *Casuarina obesa* and *Melaleuca strobophylla* on the same day is overlaid as shaded bands.

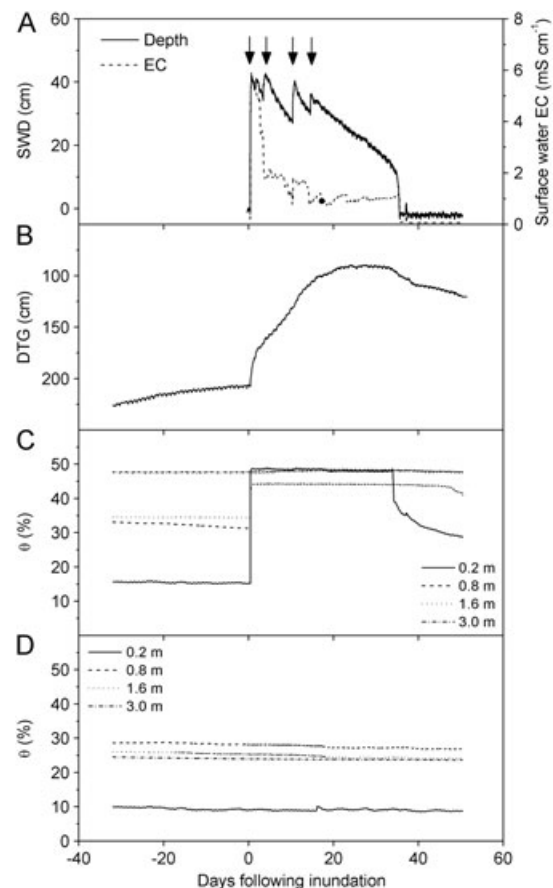


Figure 5. Surface water depth (SWD) and surface water electrical conductivity (EC) in the inundated plot (panel A). Depth to groundwater (DTG) from the soil surface beneath the inundated plot (panel B). Soil volumetric water content (θ) at 0.2, 0.8, 1.6 and 3.0 m from the soil surface within the inundated plot (panel C) and in the control plot (panel D). The arrows in panel A indicate the days when surface water was applied to the inundated plot.

surface water level within the bund declined at a rate of 9.6 mm day^{-1} and over the same period, the average reference crop evapotranspiration rate (ET_0), estimated

from climatic variables, was 2.7 mm day^{-1} . The surface water EC increased rapidly during inundation and peaked at 5.6 mS cm^{-1} (Fig. 5A). After 2 days of inundation the surface water EC had declined by more than half of this initial value and remained relatively stable throughout the remainder of the inundation period.

Logged water levels from the piezometer located within the inundated area indicated that the water table started to rise toward the surface within 3 h of applying surface water and reached a minimum value of around 90 cm, 27 days after the start of inundation (Fig. 5B). For the first 9 days of inundation, the water table beneath the inundated area trended toward the surface at a quasi steady state rate of approximately 12 mm day^{-1} . The subsequent decline in the water table coincided approximately with the eventual complete drying of surface water because of infiltration and evapotranspiration. Analysis of sub-daily fluctuations in the position of the water table revealed a semi-diurnal pattern, and this was closely associated with barometric variability and potentially some influence of evapotranspiration (data omitted). Groundwater EC beneath the bunded area was initially around 73 mS cm^{-1} , but this increased slightly to 79 mS cm^{-1} 10 days after inundation had commenced. The water table measured from a piezometer adjacent to the inundated plot rose 66 cm over the course of the experiment, reaching a minimum value of 207 cm from the ground surface 29 days after the start of inundation. The position of the water table beneath the control plot remained relatively stable throughout the experiment, declining by 32 cm.

In the inundated plot, soil volumetric water content (θ) at 0.2, 0.8 and 1.6 m from the ground surface increased rapidly within 2 h of applying water (Fig. 5C) with maximum values close to saturation (as estimated from soil particle size distribution). The increase was most marked at 0.2 m from the surface (15% to 48%). The soil volumetric water content at 3 m from the surface remained at around 48% (saturation) throughout the experiment, as the water table remained above 3 m (Fig. 5B). In the control plot θ ranged from around 9% to 28% across the soil profile but at each depth θ remained relatively stable during the experiment (Fig. 5D). Statistically, θ_v was larger in the inundated plot compared to the control plot but there was no difference on the basis of sample date (before and after inundation) and no interaction between sample date and treatment (Two-way ANOVA, Table 1).

Change in leaf water potential and plant water use during inundation

Pre-dawn leaf water potential (Ψ_{pd}) trended toward higher values during the experiment in the control, outside and inundated plots and in both species (Fig. 6). In the inundated plot, Ψ_{pd} increased significantly, relative to the initial measurement, in both species 2 days after the application of surface water (Fig. 6, repeated measures ANOVA, Table 2). Over the same period, Ψ_{pd} adjacent to the bund and in the control plot did not increase significantly in either species (Fig. 6, repeated measures ANOVA, Table 2). The average

Table 1. Two-way ANOVA comparison of maximum daily soil volumetric water content (θ).

Factor (d. f.)	F-statistic (n)	P-value
Sample date (1)	2.61 (8)	>0.05
Treatment (1)	16.01 (8)	<0.01
Sample date x treatment (1)	2.74 (4)	>0.05

Comparisons were made between sample date (before and after inundation) and treatment (control and inundated). The sampling dates were 10 March 2011 and 24 March 2011.

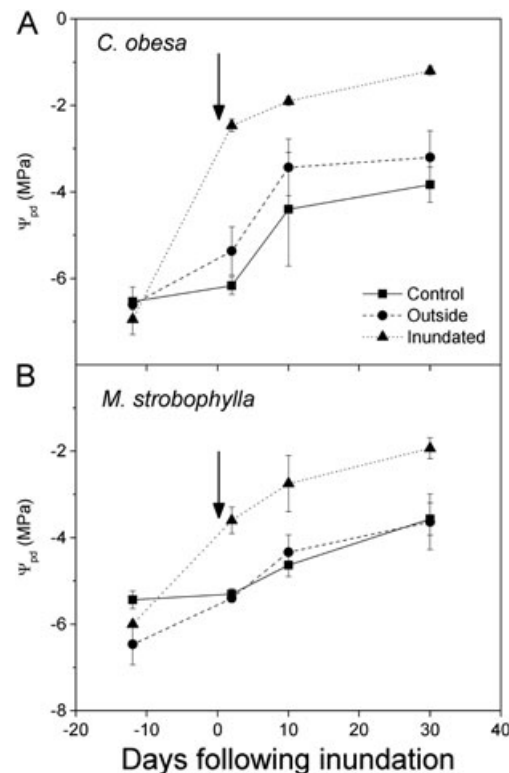


Figure 6. Pre-dawn leaf water potential (Ψ_{pd}) recorded over the study period in control, outside and inundated plots for *Casuarina obesa* (panel A) and *Melaleuca strobophylla* (panel B). The arrows indicate the day that surface water was first applied to the inundated plot.

difference in Ψ_{pd} between the inundated plot and control plot after inundation was 2.9 and 1.7 MPa for *C. obesa* and *M. strobophylla*, respectively.

Within the bunded area, sap flux (Q_s) increased the day after inundation in *C. obesa* (Fig. 7A, C and E). In contrast, Q_s was slower to increase in *M. strobophylla* (Fig. 7B, D and F). On average, Q_s increased by 3.8 and 1.2-fold in inundated *C. obesa* and *M. Strobophylla*, respectively. The increase in Q_s was paralleled by an increase in tree diameter (ϕ) in *C. obesa* and this was true, to a lesser extent, in *M. strobophylla*. In both species, there was a distinct diurnal oscillation in ϕ . Sap flux also increased in *C. obesa* outside the inundated plot (represented by Fig. 7G) but not in *M. strobophylla* (represented by Fig. 7H). In addition, there was no discernible linkage between ϕ outside of the bund area and the application of surface water (Fig. 7G and H). When comparisons were made

Table II. Repeated measures ANOVA comparison of pre-dawn leaf water potential (Ψ_{pd}) and daily sap flux (Q_s) in *Casuarina obesa* and *Melaleuca strobophylla*.

	Ψ_{pd}		Q_s	
Factor (d. f.)	F-statistic (n)	P-value	F-statistic (n)	P-value
Sample date (1)	87.81 (18)	<0.001	1.11 (18)	>0.05
Treatment (2)	6.76 (6)	<0.01	1.73 (6)	>0.05
Species (1)	0.92 (9)	>0.05	7.23 (9)	<0.05
Sample date x treatment (2)	11.1 (6)	<0.001	0.08 (6)	>0.05
Sample date x species (1)	3.17 (9)	>0.05	1.57 (9)	>0.05
Treatment x species (2)	1.10 (6)	>0.05	0.23 (6)	>0.05
Sample date x treatment x species (2)	0.53 (3)	>0.05	0.06 (3)	>0.05

Comparisons were made between sample date (before and after inundation), treatment (control, outside and inundated) and species (*C. obesa* and *M. strobophylla*). The sampling dates were 10 March 2011 and 24 March 2011.

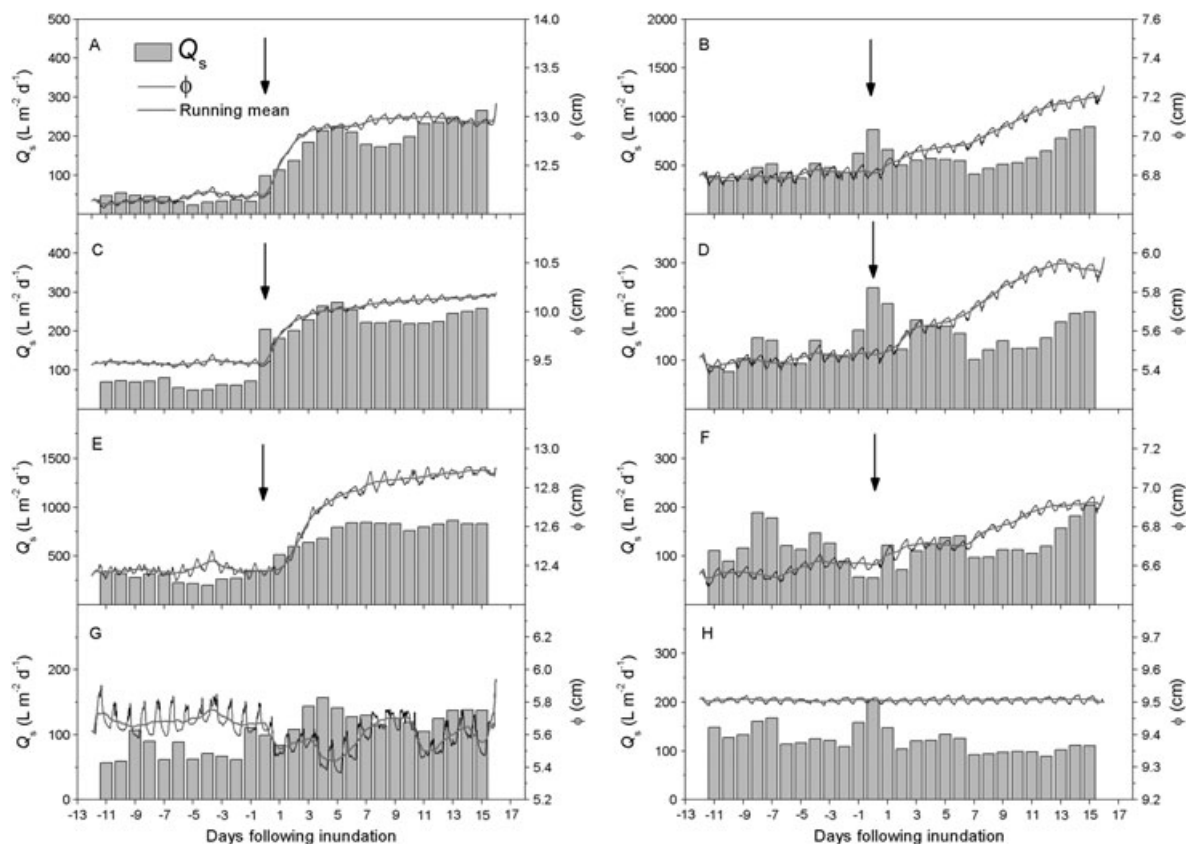


Figure 7. Daily sap flux (Q_s) and diameter recorded by point dendrometers (ϕ) from three *Casuarina obesa* trees (panels A, C and E) and three *Melaleuca strobophylla* trees (panels B, D, F) located within the inundated plot and one *C. obesa* tree (panel G) and one *M. strobophylla* tree (panel H) located in the outside plot. The arrows indicate the day that surface water was first applied. The grey line in each panel is a 48-point running mean.

before and after inundation, daily Q_s was found to be significantly larger in *M. strobophylla*, but there was no significant difference in Q_s on the basis of treatment or sampling date (repeated measures ANOVA, Table 2).

The daily stand-scale transpiration rate (E) ranged from 0.34 to 0.60 mm day⁻¹ in the control plot, 0.08 to 0.24 mm day⁻¹ in the outside plot and 0.03 to 0.13 mm day⁻¹ in the inundated plot (Fig. 8). In the outside and inundated plots, E was largest after the application of surface water. In the control plot, E fluctuated in synchrony with the reference crop evapotranspiration rate (ET_0) (Fig. 8A), and this was also the case in the outside and inundated plots prior to inundation (Fig. 8B and C).

The difference in daily maximum tree diameter between 12 days prior to inundation to 2 days after inundation ($\Delta\phi$) was positively correlated with the difference in Ψ_{pd} over the same period ($\Delta\Psi$) ($R^2=0.66$, $P<0.01$; Fig. 9). Inundated *C. obesa* trees showed the greatest increase in ϕ and Ψ_{pd} , and trees outside of the bund showed the smallest increase in ϕ and Ψ_{pd} .

DISCUSSION

To our knowledge, this is the first attempt to link changes to the soil physical environment, due to flooding, to tree water use and tree girth in a semi-arid ephemeral wetland.

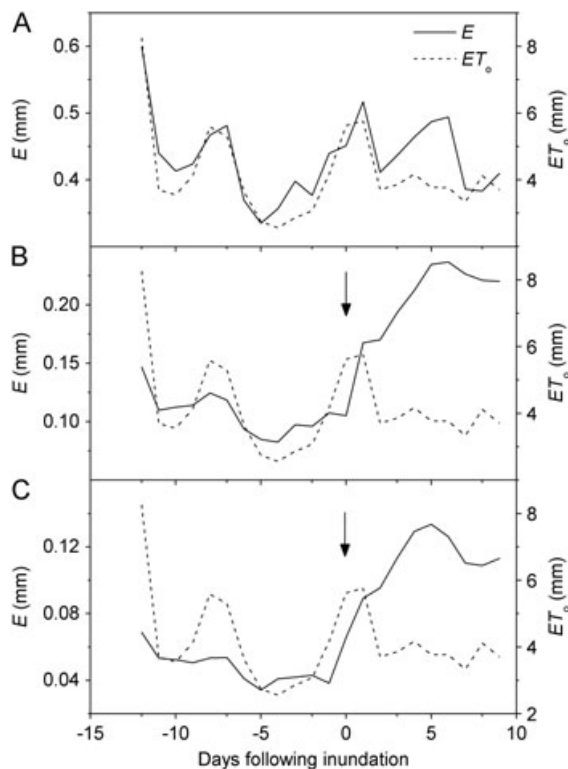


Figure 8. Daily plot-scale transpiration rate (E) and daily potential evapotranspiration rate (ET_0) in control (panel A), outside (panel B) and inundated (panel C) plots. The arrows in panel B and panel C indicate the day when surface water was first applied.

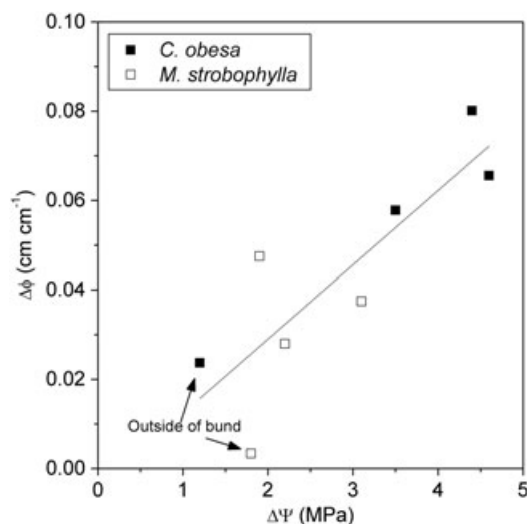


Figure 9. The relative difference in maximum daily tree diameter recorded by point dendrometers between 12 days prior to inundation and 2 days after inundation ($\Delta\phi$) was positively correlated with the difference in pre-dawn leaf water potential ($\Delta\Psi$) determined on the same days.

Inundation resulted in a rapid increase in volumetric water content (θ) throughout the unsaturated zone of the soil profile, and this was accompanied by a rise in the position of the water table (Fig. 5). Both *C. obesa* and *M. strobophylla* increased daily sap flux (Q_s) soon after inundation, but *C. obesa* was able to capitalize on the increase in θ afforded by inundation for a longer period than *M. strobophylla* (Fig. 7). There was also an increase in tree diameter (ϕ) in

both species, but this was most apparent in *C. obesa* (Fig. 7). These results are consistent with our hypothesis that the two species would respond differently to inundation because of contrasting morphological and physiological characteristics, that is, different root distributions through the soil profile. In addition, the close relationship between the presence of surface water, θ and position of the water table has implications for hydrological management at Toolibin Lake, an issue explored in the following paragraphs.

Inferred rooting depth

In theory, Ψ_{pd} and Ψ_{soil} should be in equilibrium, although we acknowledge that in our study, there was a time lag of several hours between the measurement of Ψ_{pd} and the retrieval of cores for Ψ_{soil} . Nevertheless, the inference of our leaf and soil water potential data prior to inundation is that the two species acquire water from different regions of the soil profile. At the time of measurement, *C. obesa* trees appeared to acquire water from shallow soil layers, whereas *M. strobophylla* trees were likely to have obtained water from relatively deep soil layers. Although we cannot be certain that this pattern persists throughout wet-dry seasonal cycles and during inundation events, it would appear that some form of below-ground niche separation occurs in thickets of *C. obesa* and *M. strobophylla*. This is likely to have consequences for the response of each species to changes in the soil physical environment brought about by inundation.

Change to the soil physical environment with inundation

The increase in surface water EC soon after inundation implies that some salt was mobilized from the surface soil layers and entered the bulk surface water body. The decline in surface water EC within approximately 2 days of inundation suggests that the salt that was brought into solution during the early stages of flooding quickly infiltrated into deeper soil layers. The stable EC that was recorded after 2 days of inundation is likely to closely represent the salinity of water exiting the storage tanks.

Our observation of an increase in θ in the unsaturated zone within 2 h of inundation is atypical of a soil profile dominated by clay sediments. A flow velocity of approximately 0.02 cm s^{-1} , for example, would be necessary for surface water to reach a depth of 1.6 m over this time period. Estimates of saturated hydraulic conductivity (based on particle size distribution) indicate that classical matrix (Darcian) flow is insufficient to account for such rapid water movement in clay. We believe, therefore, that the rapid increase in soil volumetric water content through the unsaturated zone is evidence of macropore flow, that is, flow of water through large continuous openings in soil (Beven and Gernann, 1982). Preferential water movement via macropores does not conform to the physical laws of Darcian flow and thus can facilitate rapid fingering flow, funnelling flow and groundwater recharge (Miyazaki, 1993). Macropore water flow velocities as large as 2 cm s^{-1} have been recorded in forest soils of New Zealand (Mosely, 1982). This is 100 times faster than the flow velocity inferred

from our study. We acknowledge that the rapid increase in θ could also be attributed to preferential movement of water down the annulus of the sensor housing tubes. However, we also detected a rapid rise in the position of the water table and increase in transpiration rate. All observations are consistent with rapid distribution of water through naturally occurring macropores.

Macropores can be morphologically characterized by the origin of their formation. In our study, the most likely origins are live or decayed roots, cracks and fissures. This is because Toolibin Lake supports dense thickets of trees and during extended dry periods, the clay profile shrinks resulting in the formation of many cracks and fissures. Macropores formed by tree roots or cracks and fissures may reduce in size as water is conveyed into the surrounding soil matrix and the clay particles swell (Bouma and Dekker, 1981; Jarvis, 2007). Thus, the rapid movement of water during inundation at Toolibin Lake may decline as the volume of macropores diminishes because of swelling of particles in the clay-dominated soil profile. In addition to the movement of water via macropore flow, water applied at the soil surface may have been hydraulically redistributed via tree roots (Burgess *et al.*, 1998), but this was not investigated in our study.

When the inputs of water ceased in the inundated area, the depth of surface water declined in a linear fashion at a rate of 9.6 mm day^{-1} . Taking into account an average potential evapotranspiration rate of 2.7 mm day^{-1} over the same period, this equates to an infiltration rate of approximately 6.9 mm day^{-1} . This is a dramatic decrease in the rate of water movement in soil inferred from changes in θ at the start of the inundation event. Such declines are typical in studies of water inputs to a system from above the soil surface (for example, Nasif and Wilson (1975)). The infiltration rate observed in the present study, being a function of gravity and the pressure forces on water at the surface, will have changed according to the rate at which water was deposited at the surface, the saturated hydraulic conductivity of soil and the degree to which soil pores were filled with water. Although we cannot attribute the attenuation of infiltration rate to any single process, it seems likely that (i) swelling reduced the effective porosity and permeability within the unsaturated zone, and (ii) a rise in the position of the water table caused percolation at depth to diminish. Both of these processes would induce a decrease in the infiltration rate at the soil surface.

The depth to the water table beneath the inundated area was tightly coupled with the presence or absence of surface water. The presence of surface water induced a steady rise in the position of the water table, and this began approximately 3 h after the first application of water. Conversely, when surface water was absent, the water table started to recede. The delay between inundation and the rise in the water table is representative of a system where lateral redistribution of water (beyond the bund area) ameliorates a rapid water table response. Significant lateral water movement within subsurface layers may have also allowed soil water in the vicinity of the surface to free drain. The EC of groundwater remained high prior to,

during, and after surface water was applied to the inundated plot. Thus, the rise in the position of the water table represents a potential incursion of highly saline groundwater into the shallow soil layers occupied by tree roots. The extent to which salt from saline groundwater diffuses upward into a profile saturated with fresh surface water requires further research, but this process is likely to be partly dependent on the depth of the water table prior to inundation. In the Toolibin Lake system, the benefits of elevating soil moisture in the unsaturated zone as a result of inundation with fresh surface water could be offset by an increase in soil salinity in the root zone because of rising saline groundwater and diffusion. The impact of these processes on tree water use will be dependent on the distribution of roots in the soil profile and the inherent tolerance of a species to salinity and water logging.

Patterns of tree water use and tree girth during inundation

There was a general increase in pre-dawn leaf water potential (Ψ_{pd}) over the study period in all plots and in both species. This was likely to be due to several small rainfall events that occurred during the experiment (totalling 9.8 mm) coupled with progressively lower temperatures (and evaporative demands). Within the inundated plot, Ψ_{pd} increased significantly compared with outside and control plots in both species 2 days after applying surface water. This confirms that some fresh surface water had entered the root zone of both species beneath the inundated area. A prolonged dry period preceded the inundation event, so this increase is likely to represent a flood-induced relaxation of xylem tension, which may have also enabled plants to operate with a higher stomatal conductance to water vapour (g_w) and transpiration rate (E) (see discussion in the following paragraphs). The sensitivity of stomata to soil water has been linked to leaf water potential (Ψ_{leaf}) (Gowing *et al.*, 1990; Tardieu and Davies, 1993; Yao *et al.*, 2001) and soil water potential (Ψ_{soil}) independent of leaf turgor (Gollan *et al.*, 1986). A sensitive stomatal response to Ψ_{soil} and/or Ψ_{leaf} is indicative of a drought resistance system configured to tightly regulate transpirational water loss. We are unaware of research comparing the relaxation time of stomatal regulation of transpiration rate during flood in ephemeral wetlands. However, in habitats characterized by episodic increases in soil water, this could be an important trait that influences growth and survival. For example, in a similar climatic zone to our study, Mitchell *et al.* (2009) observed an increase in Ψ_{pd} 10 days after a significant rainfall event in a *Eucalyptus capilliosa* woodland, and this was accompanied by a marked increase in E .

Sap flux was particularly responsive to inundation in *C. obesa*, increasing dramatically within 24 h of the addition of surface water. Several morphological and physiological characteristics could underpin this response. Firstly, *C. obesa* trees growing at Toolibin Lake are likely to be shallow-rooted, as reflected in our study and shown by work on the same species in an estuarine ecosystem by Carter *et al.* (2006). A shallow root system will quickly intercept downward-flowing water and, at Toolibin Lake,

will be less prone to the effects of rising saline groundwater. Further, macropores will typically concentrate toward the soil surface because this is where the majority of tree roots and evaporation-induced cracks occur. Emerman and Dawson (1996) showed that *Capsicum annuum* was able to survive in salinized soil because it preferentially extracted water from macropores. Macropore water in saline soil will usually be fresh because it is derived from recent rainfall or, in the case of the present study, fresh surface water. Thus, the shallow-rooted *C. obesa* trees may have been able to capitalize on fresh surface water that rapidly infiltrated the soil profile via macropores. Conversely, the more protracted response of Q_S in *M. strobophylla* is consistent with a deeper root system that receives less macropore water and is more likely to be impacted by rising saline groundwater.

A link between Q_S and ϕ was evident in trees within the inundated plot. In addition to a diurnal oscillation in ϕ , there was a trend toward larger values beginning with the application of surface water. This trend was most apparent in *C. obesa*. Changes in ϕ and Q_S are interdependent because of daily patterns of water storage and removal in stem tissue (Dobbs and Scott, 1971; Brough *et al.*, 1986; Cermak *et al.*, 2007), which are induced by fluctuations in evaporative demand. This was reflected in the diurnal oscillation of ϕ in this study, reaching a maximum value early in the morning and a minimum value between 2pm and 4pm, a pattern that is usually ascribed to changes in the water content of the elastic living tissue of bark (Zweifel and Häslar, 2001). Changes in ϕ that persist beyond diurnal fluctuations could be associated with increased cambial activity (Saveyn *et al.*, 2007; Drew *et al.*, 2008). However, we cannot conclude with certainty that the increased tree girth after inundation was more than cellular swelling.

The link between water availability and tree girth is also illustrated by the correlation between the difference in ϕ before and after inundation, and the difference in Ψ_{pd} before and after inundation. The implication of this relationship is that a greater relaxation of water stress is associated with greater increase in tree girth. Between the two species, *C. obesa* within the inundated area showed the greatest improvement in Ψ_{pd} and had the largest relative increase in ϕ . Additional research is required to verify whether the increased tree girth observed here is at least partly due to new cell formation.

Transpiration, whether expressed per unit of sapwood area (Q_S) or scaled to total plot sapwood area (E), was larger in the control plot. Trees in the control plot were, on average, larger than in the outside or inundated plots. In addition, tree density was lower in the control plot. These differences could have increased the amount of resources available to a given tree in the control plot, but this is not likely to have affected the patterns of relative change in E over the course of the study. Although daily E in the control plot was closely associated with potential evapotranspiration rate (ET_0), this was not the case in the inundated and outside plots where fluctuations in E departed from fluctuation in ET_0 after inundation. This suggests that, prior to inundation, E was limited by water availability in the root zone, but this limitation was removed after

flooding. Further, the observation that E increased outside of the bunded area suggests that lateral transmissivity of water in soil was sufficient to influence E in trees that were not directly in contact with surface water. Although not statistically significant, there was also a trend of a higher Ψ_{pd} in *C. obesa* trees adjacent to the bund after inundation.

CONCLUSIONS

The initial rate that surface water moved through the soil profile suggests that macropore flow is an important process for water distribution at Toolibin Lake. *C. obesa* was more capable than *M. Strobophylla* to capitalize on the inundation event, suggesting preferential use of macropore water and a concentration of roots near the soil surface. This could mean that the costs associated with maintaining shallow roots in ephemeral wetlands during prolonged dry spells are exceeded by the benefits of access to fresh water derived from episodic flood events. The fact that species with different root architectural arrangements coexist suggests that competition for below-ground resources in semi-arid ephemeral wetlands is a driver for adaptation. Under normal circumstances, these different strategies would result in a relatively stable plant community assemblage. However, rising saline groundwater due to secondary salinity will disadvantage deeper-rooted species, and this could result in the dominance of shallow-rooted species such as *C. obesa*.

Sap flux and ϕ were interdependent, and there was a correlation between increasing ϕ and increasing Ψ_{pd} . Hence, the movement of surface water through the soil profile has predictable outcomes for tree water use and tree girth at Toolibin Lake. Changes in the soil physical environment observed in this study also reveal important risks associated with hydrological interventions by operational managers in salinity-affected ecosystems. Although floods have the potential to provide fresh water to the root zone of trees through infiltration processes, they also carry the risk of bringing saline groundwater into the zone of plant water uptake through recharge. Further research is required to determine whether the observations of this study are replicated when an inundation event is preceded by a wet period as opposed to an extended dry period.

ACKNOWLEDGEMENTS

This project was financially supported by the Future Farm Industries Cooperative Research Centre (FFI CRC). Thanks to Darren Farmer, Ray McKnight, Maria Lee, Jen Higbid, Jon Waters and Rachael Wroe for technical assistance and to Ken Wallace, Gary Ogden and Ray Froend for helpful comments. Two anonymous reviewers provided constructive feedback on an earlier version of this manuscript.

REFERENCES

- Australian Bureau of Meteorology. 2010. Climate Averages for Western Australia. Canberra, A CT, Australia.

- Allen, RG, Pereira LS, Raes D, Smith M (1998). Crop evapotranspiration – guidelines for computing crop water requirements – FAO irrigation and drainage paper 56. Rome, United Nations.
- Bell DT 1999. Australian trees for the rehabilitation of waterlogged and salinity-damaged landscapes. *A. J. Bot.* **47**: 697–716.
- Beven K, Gernann P 1982. Macropores and water flows in soils. *Water Resources Research* **18**: 1311–1325.
- Bouma J, Dekker LW 1981. A method for measuring the vertical and horizontal k_{sat} of clay soils with macropores. *Soil Science Society of America Journal* **45**: 662–663.
- Brough DW, Jones HG, Grace J 1986. Diurnal changes in water content of the stems of apple trees, as influenced by irrigation. *Plant, Cell & Environment* **9**: 1–7.
- Burgess SSO, Adams MA, Turner NC, Ong CK 1998. The redistribution of soil water by tree root systems. *Oecologia* **115**: 306–311.
- Burgess SSO, Adams MA, Turner NC, Beverly CR, Ong CK, Khan AAH, Bleby TM 2001. An improved heat pulse method to measure low and reverse rates of sap flow in woody plants. *Tree Physiology* **21**: 589–598.
- Carter JL, Veneklaas EJ, Colmer TD, Eastham J, Hatton TJ 2006. Contrasting water relations of three coastal tree species with different exposure to salinity. *Physiol. Plantarum* **127**: 360–373.
- Cermak J, Kucera J, Bauerle WL, Phillips N, Hinckley TM 2007. Tree water storage and its diurnal dynamics related to sap flow and changes in stem volume in old-growth Douglas-fir trees. *Tree Physiology* **27**: 181–198.
- Cowan IR 1977. Stomatal behaviour and environment. *Advances in Botanical Research* **4**: 117–228.
- Dobbs RC, Scott DRM 1971. Distribution of diurnal fluctuations in stem circumference of Douglas fir. *Can. J. Forest Res.* **1**: 80–83.
- Drew DM, O'Grady AP, Downes GM, Read J, Worledge D 2008. Daily patterns of stem size variation in irrigated and unirrigated *Eucalyptus globulus*. *Tree Physiology* **28**: 1573–1581.
- El-Lakany MH, Luad EJ 1983. Comparative salt tolerance of selected *Casuarina* species [Australia; Egypt]. *A. J. Forest Res.* **13**: 11–20.
- Emerman SH, Dawson TE 1996. The role of macropores in the cultivation of bell pepper in salinized soil. *Plant and Soil* **181**: 241–249.
- Farquhar GD, Sharkey TD 1982. Stomatal conductance and photosynthesis. *Annu. Rev. Plant Phys.* **33**: 17–45.
- Fennessy MS, Cronk JK, Mitsch WJ 1994. Macrophyte productivity and community development in created wetlands under experimental hydrological conditions. *Ecological Engineering* **3**: 469–484.
- George RJ, McFarlane DJ, Nulsen RA 1997. Salinity threatens the viability of agriculture and ecosystems in Western Australia. *Hydrogeology Journal* **5**: 6–21.
- George RL, Dogramaci S 2000. Toolibin – a life and death struggle for the last freshwater Wheatbelt lake. Proceedings of the Third International Hydrology and Resources Conference, Perth.
- Gollan T, Passioura JB, Munns R 1986. Soil water status affects the stomatal conductance of fully turgid wheat and sunflower leaves. *A. J. Plant Physiol.* **13**: 1–7.
- Gowing DJG, Davies WJ, Jones HE 1990. A positive root-sources signal as an indicator of soil drying in apple, *Malus x Domestica*-Borkh. *Journal of Experimental Botany* **41**: 1535–1540.
- Hurlbert SH. 1984. Pseudoreplication and the design of ecological field experiments. *Ecological Monographs* **54**: 187–211.
- Jackson RB, Pockman WT, Hoffmann WA 1999. The structure and function of root systems. *Handbook of Functional Plant Ecology*. Pugnaire FI, Valladares F Marcel Dekker: Basel; 195–220.
- Jarvis NJ 2007. A review of non-equilibrium water flow and solute transport in soil macropores: principles, controlling factors and consequences for water quality. *European Journal of Soil Science* **58**: 523–546.
- Kawase M 1981. Anatomical and morphological adaptation of plants to waterlogging. *HortScience* **16**: 30–34.
- Mitchell PJ, Vaneklaas E, Lambers H, Burgess SO 2009. Partitioning of evapotranspiration in a semi-arid eucalypt woodland in south-western Australia. *Agr. Forest Meteorol.* **149**: 25–37.
- Mosely MP 1982. Subsurface flow velocities through selected forest soils, South Island, New Zealand. *Journal of Hydrology* **55**: 65–92.
- Miyazaki T 1993. *Water Flow in Soil*. New York: Marcel Dekker Inc.
- Nasif SH, Wilson EM 1975. The influence of slope and rain intensity on runoff and infiltration. *Hydrol. Scie. Bull.* **20**: 539–553.
- Neill C 1990. Effects of nutrients and water levels on emergent macrophyte biomass in a prairie marsh. *Canadian Journal of Botany* **68**: 1007–1014.
- Oksanen L 2001. Logic of experiments in ecology: is pseudoreplication a pseudoissue? *Oikos* **94**: 27–38.
- Saveyn A, Steppe K, Lemeur R 2007. Daytime depression in tree stem CO₂ efflux rates: is it caused by low stem turgor pressure? *Annals of Botany* **99**: 477–485.
- Scholander, PF, Hammel HT, Hemmingsen EA, Bradstreet ED 1964. Hydrostatic pressure and osmotic potential in leaves of mangroves and some other plants. *P. Natl. Acad. of Sci.* **52**: 119–125.
- Sorrell BK, Mendelssohn IA, McKee KL, Woods RA 2000. Ecophysiology of wetland plant roots: a modelling comparison of aeration in relation to species distribution. *Annals of Botany* **86**: 675–685.
- Tanner W, Beevers H 2001. Transpiration, a prerequisite for long-distance transport of minerals in plants? *P. Natl. Acad. of Sci.* **98**: 9443–9447.
- Tardieu F, Davies WJ 1993. Integration of hydraulic and chemical signalling in the control of stomatal conductance and water status of droughted plants. *Plant, Cell & Environment* **16**: 341–349.
- Tombjerg T, Bendix M, Brix H 1994. Internal gas transport in *Typha latifolia* L. and *Typha angustifolia* L. 2. Convective throughflow pathways and ecological significance. *Aquatic Botany* **49**: 91–105.
- Touchette BW, Iannaccone LR, Turner G, Frank A 2010. Ecophysiological responses of five emergent-wetland plants to diminished water supply: an experimental microcosm study. *Aquatic Ecology* **44**: 101–112.
- Whigham DF 1999. Ecological issues related to wetland preservation, restoration, creation and assessment. *Science Tot. Environ.* **240**: 31–40.
- Yao C, Moreschet S, Aloni B 2001. Water relations and hydraulic control of stomatal behaviour in bell pepper plant in partial soil drying. *Plant, Cell & Environment* **24**: 227–235.
- Zweifel R, Häslér R 2001. Dynamics of water storage in mature subalpine *Picea abies*: temporal and spatial patterns of change in stem radius. *Tree Physiology* **21**: 516–569.